

# Investigation of spin dynamics in a magnetically diluted crystal by the enhanced susceptibility technique

E. V. Avagyan, V. A. Atsarkin, and G. A. Vasneva

*Institute of Radio Engineering and Electronics, USSR Academy of Sciences*

(Submitted 5 May 1983)

Zh. Eksp. Teor. Fiz. **85**, 1790–1800 (November 1983)

The establishment and relaxation of spin-spin temperature in magnetically diluted  $\text{TiO}_2:\text{Cr}^{3+}$  crystals are investigated by the enhanced-susceptibility effect. The experiments are performed in a zero magnetic field with microwave pumping near the initial splitting of  $\text{Cr}^{3+}$  at liquid-helium temperature. The effect is observed in a detuning range that exceeded the EPR line width by 2–3 orders of magnitude, thus indicating that the line has rather extended wings. It is established that the return of the spin-spin subsystem to equilibrium after turning off the microwave pump is not described by a single exponential and depends on the frequency of the microwave-field and on the duration of its action on the sample. These anomalies are interpreted as a manifestation of the spectral diffusion in an EPR line broadened by spin-spin interactions between the paramagnetic centers that are randomly distributed over the volume. It is suggested that in a magnetically diluted system such a broadening is essentially inhomogeneous and that the spectral diffusion that lasts for a time up to  $10^{-3}$  sec constitutes formation of a quasi-equilibrium spin-spin reservoir.

PACS numbers: 76.30.Fc

## 1. INTRODUCTION

The physical picture of dynamic and relaxation processes in magnetically dilute solids is far from completely clear. Too little is known concerning such fundamental processes as the distribution and correlation of the local fields, the rate of the spin-spin flips, the establishment and relaxation of spin temperatures, and others. Of great use in the experimental study of these problems can be the method of enhanced susceptibility,<sup>1</sup> which has given very good account of itself in experiments with ruby crystals.<sup>2–5</sup>

One of the most convenient variants of the enhanced-susceptibility method is one with zero magnetic field  $H_0 = 0$  and microwave pumping near the frequency  $\nu_0$  of the “initial splitting” of the energy levels of a paramagnetic center with spin  $S > 1/2$ .<sup>4</sup> This is precisely the technique used in the present study, the objects of the investigation being crystals of rutile  $\text{TiO}_2$  doped with  $\text{Cr}^{3+}$  ions. Before we proceed to an exposition of the experimental results, let us recall, with rutile as the example, the physical gist and the main features of the method.<sup>1</sup>

In a zero magnetic field the single-frequency spin Hamiltonian of a  $\text{Cr}^{3+}$  ion in rutile is

$$\mathcal{H}_s = D(S_z^2 - S^2/4) + E(S_x^2 - S_y^2), \quad (1)$$

where  $S = 3/2$ ;  $D = -0.68 \text{ cm}^{-1}$ ,  $E = -0.14 \text{ cm}^{-1}$ , and the coordinate system  $(x, y, z)$  is determined by the principal magnetic axes of the  $\text{Cr}^{3+}$  ions.<sup>7</sup> The corresponding energy spectrum consists of two Kramers doublets separated by an interval  $\nu_0 \approx 43 \text{ GHz}$ . The energy subsystem corresponding to the Hamiltonian (1) will be referred to as the “Stark” subsystem (to distinguish it from the “Zeeman” subsystem produced by an external magnetic field).

The spin-spin interactions  $\mathcal{H}_{SS}$  between paramagnetic centers (more accurately, their secular part  $\mathcal{H}'_{SS}$ , i.e., the

one commuting with  $\mathcal{H}_s$ ), make up a separate subsystem—the electronic spin-spin reservoir (ESSR). It is usually assumed that it is in an internal-equilibrium state with a temperature  $T_{SS} = 1/\beta_{SS}$ .<sup>8,9</sup>

A weak probing field  $h \cos \Omega t$  is applied to the sample and is used to measure the low-frequency magnetic susceptibility  $\chi(\Omega)$ . The latter is due to the magnetization by the Zeeman splitting of each of the Kramers doublets in the field  $h \cos \Omega t$ . Since this field is much weaker than the local one, the Zeeman energy of the doublets is mixed with the ESSR and acquires its temperature  $T_{SS}$ . Therefore  $\chi(\Omega) \propto \beta_{SS}$ , so that measurement of the low-frequency susceptibility permits  $\beta_{SS}$  to be directly determined and its evolution tracked.

The proportionality of  $\chi(\Omega)$  and  $\beta_{SS}$  can be explained also in other terms. The imaginary part  $\chi''(\Omega)$  of the susceptibility is the coefficient of absorption of the low-frequency field by the spin system. This absorption is due to transitions induced in the ESSR spectrum by the field  $h \cos \Omega t$ . They are allowed because at  $H_0 = 0$  the secular parts of the spin-spin interactions include terms of the type  $S_z S_{\pm}$ . Naturally, therefore,  $\chi''(\Omega) \propto 1/T_{SS}$ .

Turning on the microwave pump, which saturates the EPR near the frequency  $\nu_0$ , causes strong cooling of the ESSR,<sup>8,9</sup> and hence an increase of  $|\chi(\Omega)|$  (the enhanced-susceptibility effect). From the magnitude of the effect we can, in particular, determine the mean squared local field  $\omega_{SS}$ . After turning off the microwave pump, the signal  $\chi(\Omega)$  returns to its equilibrium value. Observation of this process was used to obtain information on the ESSR spin-lattice relaxation, as well as on the coupling of the ESSR and the spin system of the matrix nuclei in ruby crystals.<sup>3,4</sup>

We note that, unlike ruby, the  $\text{TiO}_2$  lattice contains only a small number of nuclei with spin. These are the low-abundance isotopes  $^{47}\text{Ti}$  and  $^{49}\text{Ti}$ , which furthermore have very small magnetic moments. Therefore the coupling of the

TABLE I. Parameters of investigated samples and summary of experimental results.

c	$\delta_{1/2}$ , MHz	$T_L$ , K	$\Delta_{max}^0$ , MHz	$\Delta_{max}^\infty$ , MHz	$a_{exp}$	$\tau_{SSL}$ , msec
0.05%	7.0	1.65	75	195	7.0±1	5.8
		4.2	60±10	170	8.0±2	2.0
0.2%	12.5	1.65	190±40	550	8.3±2	1.0
		4.2	-	400	-	0.35

ESSR with the nuclear spin system is here very weak and can hardly influence substantially the behavior of the electronic spin-spin reservoir. For the same reason, broadening of the rutile EPR lines by hyperfine interactions with the matrix nuclei is practically nonexistent.

These circumstances make the  $TiO_2:Cr^{3+}$  crystals very convenient objects for our investigations.

2. EXPERIMENT

The experiments were performed at temperatures  $T_L = (1.65-4.2)$  K on  $TiO_2$  crystals with  $Cr^{3+}$  densities  $c = (0.05-0.2)\%$ , corresponding to  $n = (1.5-6.0) \times 10^{19}$   $cm^{-3}$  paramagnetic centers. The basic measurements were made on samples with minimum and maximum density. Their parameters are listed in the table. (In the cases when the measurement error is not indicated, it equals 10%;  $c$  was measured by the EPR method;  $\delta_{1/2}$  is the half-width at half maximum of the intensity of the EPR line corresponding to the  $\pm 1/2$  transition at  $H_0 || z$  in the 3-cm wavelength band.)

The experimental technique hardly differed from that described in Ref. 4. The susceptibility  $\chi(\Omega)$  was measured at a frequency  $\Omega/2\pi \approx 2$  MHz, so that the condition  $\delta_{1/2} > \Omega \gg \tau_{SL}^{-1}$  was satisfied, where  $\delta_{1/2}$  is the half-width of the EPR line at half intensity and  $\tau_{SL} \sim (10^{-3} - 10^{-2})$  sec is the spin-lattice relaxation time of the Stark subsystem.

A typical experimental oscillogram is shown schematically in Fig. 1. The region I corresponds to a growth of the enhanced susceptibility as the EPR saturates. This process concludes at the instant  $t_0$ , when the susceptibility reaches a maximum. Region II is the transition to a stationary regime ("plateau" on Fig. 1). Finally, when the microwave pump is

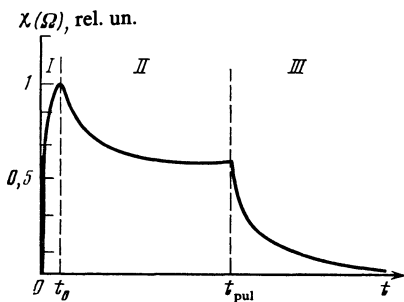


FIG. 1. Change of low-frequency susceptibility  $\chi(\Omega)$  under the action of a microwave pump pulse. The pulse was turned on at the instant  $t = 0$  and off at  $t = t_{pul}$ . Roman numerals mark the main stages of the transition process (see the text).

turned off the signal  $\chi(\Omega)$  returns to the equilibrium value  $\chi_L(\Omega)$  (region III).

Figures 2 and 3 show the enhancement coefficient  $E = \chi(\Omega)/\chi_L(\Omega)$  of the susceptibility as a function of the microwave pump frequency  $\nu_p = \nu_0 + \Delta$  at  $T_L = 1.65$  K. The measurements were performed both at the instant  $t_0$  and in the stationary regime.

Most experimental points were obtained under conditions of strong saturation of the EPR, but in measurements of the susceptibility at the instant  $t_0$  at  $c = 0.2\%$  the microwave source power was insufficient for saturation and we used a suitable extrapolation. The error in this case was noticeably higher.

The equilibrium  $\chi_L(\Omega)$  signal was very weak, so that the scale of the absolute values of  $E$  was initially set at a low accuracy ( $\pm 50\%$ ).

It can be seen from Figs. 2 and 3 that the experimental results are satisfactorily described by the known formula of the spin-temperature theory<sup>8,9</sup>

$$E = \frac{\beta_{ss}}{\beta_L} = - \frac{\nu_0 \Delta}{\Delta^2 + \Delta_{max}^2}, \tag{2}$$

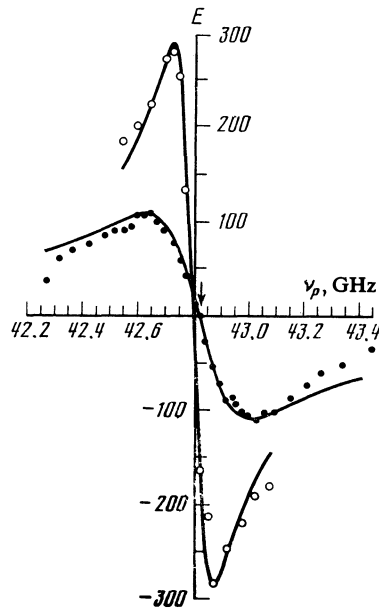


FIG. 2. Dependence of the susceptibility-enhancement coefficient  $E$  on the pump frequency  $\nu_p$ . Light circles—results of measurements at the instant  $t_0$ , dark—in the stationary regime, curves—calculation by Eq. (2). The arrow marks the singular point (see the text).  $T_L = 1.65$  K;  $c = 0.05\%$ .

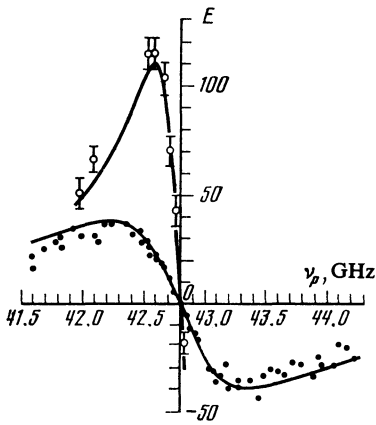


FIG. 3. The same as in Fig. 2, but for  $c = 0.2\%$ .

where  $\beta_L = 1/T_L$  and  $\Delta_{\max}$  is that detuning  $|\Delta|$  at which the enhancement reaches its external values  $\pm E_{\max}$ . The parameters  $\Delta_{\max}^0$  and  $\Delta_{\max}^\infty$  obtained experimentally in this manner for  $T_L = 1.65$  K and 4.2 K are given in the table (here and elsewhere all the quantities pertaining to the instant  $t_0$  are marked by a superscript  $0$ , while those for the stationary regime are labeled  $\infty$ ).

According to the prevailing notions<sup>8,9</sup>  $\Delta_{\max}^0 = \omega_{SS}$  and  $\Delta_{\max}^\infty = \omega_{SS} a^{1/2}$ , where  $a = \tau_{SL}/\tau_{SSL}$  and  $\tau_{SSL}$  is the spin-lattice relaxation time of the ESSR. From the experimental plots of  $E^0(\nu_p)$  and  $E^\infty(\nu_p)$  we can thus obtain the values

$$a_{\text{exp}} = (\Delta_{\max}^\infty/\Delta_{\max}^0)^2 = (E_{\max}^0/E_{\max}^\infty)^2.$$

They are also listed in the table.

Substitution of the experimental  $\Delta_{\max}$  in (2) was used next for a final calibration of the enhancement coefficient  $E$  (the ordinate scales of Figs. 2 and 3).

We defer the discussion of these results to the next section, and note for the time being that the obtained values  $a_{\text{exp}} = 6$  to 10 turned out to be unexpectedly large. We note also the strikingly large range of detunings  $\Delta$  in which the susceptibility enhancement is observed: for  $c = 0.2\%$ , e.g., it spans at least several GHz (Fig. 3). This means that the EPR line has quite long wings whose spans exceed its half-width by two or three orders of magnitude (see the table).

A curious feature of Fig. 2 is a small but incontroverti-

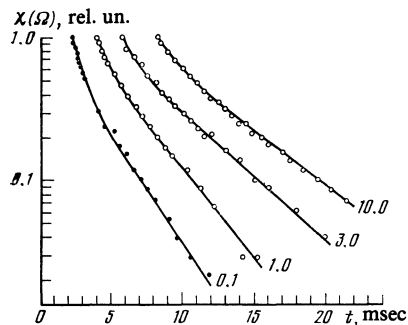


FIG. 4. Return of the signals  $\chi(\Omega)$  to equilibrium after turning off microwave pulses of various durations (the values of  $t_{\text{pul}}$  in milliseconds are marked on the curves). The start of each curve corresponds to the instant when the pulse is turned off;  $T_L = 1.65$  K;  $c = 0.05\%$ ;  $\Delta = -125$  MHz.

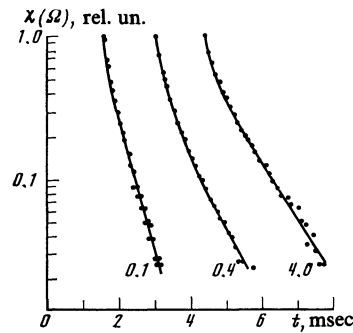


FIG. 5. The same as in Fig. 4, but for  $c = 0.2\%$  and  $\Delta = -330$  MHz.

ble shift of the point  $E = 0$  on going from the instant  $t_0$  to a stationary regime. It is known that this point corresponds to the "center of gravity" of the EPR line, i.e., to the initial splitting frequency  $\nu_0$ . We note incidentally that the quantity  $\nu_0$  determined in this manner from Figs. 2 and 3 amounts to  $(42.81 \pm 0.02)$  GHz, which differs somewhat from the published<sup>7</sup> value  $(43.3 \pm 0.2)$  GHz.

A study of the ESSR relaxation after turning off the microwave pump yielded even more unexpected results. In the entire investigated range of  $c$  and  $T_L$  the return of the  $\chi(\Omega)$  signal to equilibrium was substantially nonexponential. Some relaxation curves are shown in Figs. 4 and 5. It can be seen that all have a rapid nonexponential initial section. At a fixed value of  $\Delta$  the rate of relaxation increases noticeably with decreasing duration  $t_{\text{pul}}$  of the microwave pulse. On the contrary, with increasing  $t_{\text{pul}}$  the dominant role is assumed by the relatively slow exponential "tail" whose characteristic time tends to a certain limiting value. We have taken it to be the ESSR spin-lattice relaxation time. Data on the temperature and density dependences of  $\tau_{SSL}$  are given in the table.

At a fixed  $t_{\text{pul}}$  the amplitude of the rapid initial section increases as the center of the EPR line is approached and reaches a maximum at a "singular point"  $\nu_p = 42.825$  GHz, where  $E^0 < 0$  and  $E^\infty = 0$  (see Fig. 2). The corresponding relaxation curve for  $c = 0.05\%$  is shown in Fig. 6. Here practically the entire decay takes place within a very short time of the order of  $0.5 \text{ msec} \ll \tau_{SSL}$ . A similar time dependence of the susceptibility is observed at the singular point also in the

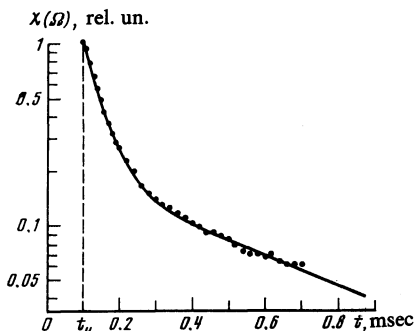


FIG. 6. Relaxation of the  $\chi(\Omega)$  signal at the singular point (see the text).  $T_L = 1.65$  K;  $c = 0.05\%$ ;  $t_{\text{pul}} = 0.1$  msec. Solid curve—sum of two exponentials with time constants  $5.5 \times 10^{-5}$  and  $6.5 \times 10^{-4}$  sec.

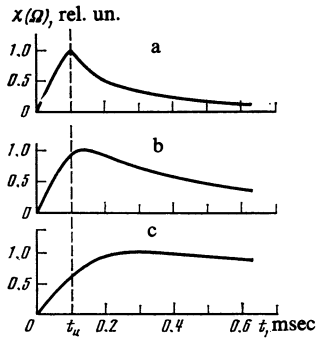


FIG. 7. Buildup and relaxation of  $\chi(\Omega)$  signals at  $T_L = 1.65$  K;  $c = 0.2\%$  and at different values of the pump frequency: a)  $\Delta = -50$  MHz; b)  $\Delta = -640$  MHz; c)  $\Delta = -2.5$  GHz. The vertical dashed line corresponds to turning off the microwave pulse.

presence of saturation of the microwave field, i.e., in region II of Fig 1.

With increasing  $|\Delta|$  the amplitude of the fast part of the relaxation decreases, and at short microwave pulses and very large detunings it even reverses sign (Fig. 7). This means that immediately after turning off the pulse the signal  $\chi(\Omega)$  still continues to increase and only later does it begin to fall off (Fig. 7b). The relaxation “delay” time increases with increasing detuning and is about 0.2 msec at  $c = 0.2\%$  and  $|\Delta| \approx 3$  GHz.

We were unable to find a universal analytic expression capable of describing the relaxation kinetics at all values of  $t_{\text{pul}}$  and  $\Delta$ . In certain cases the relaxation curves are satisfactorily described by a sum of two exponentials (Fig. 6). Given  $t_{\text{pul}}$  and  $\Delta$ , the rate of the faster of them depends little on temperature and is approximately proportional to the chromium concentration.

### 3. DISCUSSION OF RESULTS

#### a. Spectral diffusion and thermal mixing

It is most natural to attribute the anomalies noted in the preceding section to spin-spin cross relaxation which leads to spectral diffusion of the saturation over the EPR line. This process can also be regarded as thermal mixing between the spin-spin reservoir cooled by the microwave pumping and the so-called “difference” subsystems 9–11 that are made up of the spin packets contained in the line. The mixing produces a new quasi-equilibrium subsystem—the local-field reservoir (LFR).<sup>12,9</sup> Its specific heat is much larger than that of the ESSR. It is the distribution of the energy initially stored in the ESSR over the entire LFR which causes the relatively rapid decrease of  $|\beta_{SS}|$  after short microwave pulses (Figs. 4–6).

If the pulse duration  $t_{\text{pul}}$  exceeds the characteristic cross-relaxation time  $\tau_{\text{cr}}$ , the mixing is completed mainly during the time of the pulse and is therefore manifest to a lesser degree after the pulse end. This explains the apparent slowing down of the relaxation with increase of  $t_{\text{pul}}$  (Figs. 4 and 5), which was observed many times in systems with cross relaxation and spectral diffusion.<sup>13,14</sup>

We discuss now the anomalously high values of  $a_{\text{exp}} = (\Delta_{\text{max}}^{\infty} / \Delta_{\text{max}}^0)^2 \approx 8 \pm 2$  (see the table). We recall that if

the spin-lattice relaxation of the ESSR proceeds via the proper Stark subsystem of the  $\text{Cr}^{3+}$  ions, the theory predicts  $a_{\text{theor}} = \tau_{SL} / \tau_{SSL} \approx 1$  at  $H_0 = 0$  (Ref. 4). To be sure, this quantity can be substantially increased by rapidly relaxing foreign impurities,<sup>4</sup> but such a mechanism is hardly compatible with the almost linear variation of  $\tau_{SSL}^{-1}$  as a function of  $T_L$  and with the practical absence of a density dependence of  $a_{\text{exp}}$  (compare the table with the results for ruby 4). Finally, a comparison of our values of  $\tau_{SSL}$  with the published data<sup>15</sup> on the time  $\tau_{SL}$  yields  $\tau_{SL} / \tau_{SSL} \approx 1 - 3$ , which is also much lower than  $a_{\text{exp}}$ .

This discrepancy, however, can be explained by assuming that  $\tau_{\text{cr}} \gg t_0$ , so that on going from  $t_0$  to a stationary regime the effective specific heat of the ESSR is increased because of difference subsystems added to it. Taking this factor into account, we have

$$(\Delta_{\text{max}}^{\infty})^2 = \frac{\tau_{SL}}{\tau_{SSL}} \omega_{SS}^2 + \frac{\tau_{SL}}{\tau_{\delta L}} M_2, \quad (3)$$

where  $\tau_{\delta L}$  is the time of the spin-lattice relaxation of the difference subsystems (usually assumed equal to  $\tau_{SL}$ ), and  $M_2$  is the second moment of the spin distribution over the packets. Since the EPR line has very long wings,  $M_2$  is large and the second term in the right-hand side of (3) brings about the experimentally observed relation  $a_{\text{exp}} = (\Delta_{\text{max}}^{\infty} / \omega_{SS})^2 > \tau_{SL} / \tau_{SSL}$ .

The shift of the point  $E = 0$  (Fig. 2) can also be interpreted within the framework of the same model. It appears that the “joining” of its far wings to the EPR line shifts slightly ( $\sim 25$  MHz) its center of gravity. Understandably, even a very weak asymmetry of wings that span hundreds and thousands of MHz can lead to an observable effect.

We turn finally to the dependence of the shapes of the relaxation curves on the detuning  $\Delta$  (Fig. 7). It can be qualitatively attributed to the fact that with increasing  $|\Delta|$  direct cooling of the difference subsystems by the microwave field becomes increasingly more significant. Under these conditions the thermal mixing no longer leads to a substantial decrease of  $|\beta_{SS}|$ , and at very large detunings it might even contribute to its growth.

This statement may not seem obvious enough, and we shall consider this question in greater detail.

The Hamiltonian of an assembly of difference subsystems is

$$\mathcal{H}_{\delta} = \sum_j S_{zj} \delta_j,$$

where the summation is over all the spin packets with frequencies  $\nu_j = \nu_0 + \delta_j$ , while  $\sum \delta_j = 0$ . A short microwave pulse of duration  $t_{\text{pul}} \approx t_0 \ll \tau_{\text{cr}}$  saturates the  $p$ -th packet, for which  $\delta_p = \Delta$ . As a result the corresponding difference subsystem  $\mathcal{H}_{\Delta}$  is cooled whereas all the remaining (“passive”) difference subsystems remain at the lattice temperature.<sup>11</sup>

What is also cooled, of course, is the ESSR. Its temperature at the instant  $t_{\text{pul}}$  can be obtained from the formulas of Refs. 16 and 17, which correspond to “hole burning” in the EPR line without allowance for spectral diffusion.

After the termination of the pulse, thermal mixing begins. We list below the subsystems that participate in this

process, and cite for each in succession the Hamiltonian, the reciprocal temperature at the end of the pulse, and the specific heat  $c_i$  (in relative units).<sup>11,16,17</sup>

1) ESSR:

$$\mathcal{H}_{SS}'; \quad \beta_{SS} \approx \alpha \beta_L \nu_0 g'(\Delta) / g(\Delta); \quad c_{SS} = \omega_{SS}^2. \quad (4)$$

2) "Active" ( $p$ -th) difference subsystems:

$$\mathcal{H}_\Delta = S_{zp} \Delta; \quad \beta_\Delta^0 \approx -\beta_L \nu_0 / \Delta; \quad c_\Delta = \alpha \Delta^2. \quad (5)$$

3) "Passive" difference subsystems:

$$\mathcal{H}_\delta^0 = \sum_{j \neq p} S_{zj} \delta_j; \quad (\beta_\delta^0)^0 = \beta_L; \quad c_\delta^0 \approx M_2. \quad (6)$$

Here  $\alpha$  is the fraction of the spins subjected to saturation;  $g(\Delta)$  and  $g'(\Delta)$  are the EPR line shape and its derivative at the point  $\Delta$ . It is assumed that  $\alpha \ll 1$  and the width of the "hole" is of the order of  $\omega_{SS}$ .

The reciprocal temperature established in the LFR as a result of the mixing is

$$\beta_{SS} = \sum_i \beta_i^0 c_i / \sum_i c_i. \quad (7)$$

Substituting (4)–(6) in (7) it is easy to verify that if the EPR line wings do not fall off too steeply the quantity

$$\eta = (\beta_{SS}^0 - \tilde{\beta}_{SS}^0) / \beta_{SS}^0,$$

which describes the amplitude of the rapid initial section of the relaxation curve, decreases with increasing  $|\Delta|$ , and reverses sign at very large detunings. In particular, for a truncated Lorentz curve we have  $\eta \approx 1 - \Delta^2 / M_2$ , so that delay of the relaxation should set in at  $|\Delta| > M_2^{1/2}$ . This is indeed observed in experiment (Fig. 7c).

We note that the entire aggregate of the experimental data cannot be explained even qualitatively as being due to other possible causes of the nonexponential relaxation of the ESSR. These include departure from the framework of high-temperature approximation (in our case  $h\nu_0/kT_L \approx 1.2$ ), the coupling of the ESSR with the nuclear spin system of the matrix, the phonon bottleneck, or the spectral asymmetry of the spin-phonon interaction.<sup>18,19</sup> We note also that the content of the foreign paramagnetic impurities that give rise to an EPR spectrum (e.g.,  $\text{Fe}^{3+}$ ) amounted in our samples to less than 1% of the  $\text{Cr}^{3+}$  content.

## b. The spin-spin inhomogeneous-broadening hypothesis

There are therefore all grounds for assuming that we have actually observed manifestations of spectral diffusion, and that the characteristic times of this process lie in the range ( $3 \cdot 10^{-5} - 3 \cdot 10^{-3}$ ) sec (the lower limit is determined by the temporal resolution of our apparatus, and the upper by the time  $\tau_{SSL}$ ). This means that the EPR line in the investigated samples behaves as an inhomogeneously broadened one. But what is the character of this inhomogeneous broadening?

It can be seen from the table that the line width at half intensity increases with the concentration and is close at  $c = 0.2\%$  to the dipole value  $\delta_d$  (Ref. 20). Increasing with  $c$  is also the quantity  $\Delta_{\max}^\infty$  that characterizes the specific heat of the LFR. All this offers evidence that such traditional causes

of inhomogeneous broadening as crystal imperfections, hyperfine interactions with the matrix nuclei, and others do not play a significant role here.

On the other hand, the statistical theory of spin-spin line broadening in magnetically dilute solids predicts the existence of quite extended and relatively slowly drooping wings.<sup>20</sup> In ruby they were observed in experiment even up to detunings on the order of 30 GHz.<sup>21</sup> These far line wings comprise the spectrum of like paramagnetic centers which, owing to their random distributions in the volume, are quite close to one another and are therefore in relatively strong local fields. We call these "cluster" centers. On the other hand, the central part of the EPR line, which is the one usually observed by radiospectroscopists, is made up of "solitary" spins, which have no neighbors at an average distance  $\bar{r} = n^{-1/3}$ .

In accord with a tradition stemming from NMR spectroscopy, spin-spin broadening is regarded as homogeneous, and the time to establish internal quasi-equilibrium is assumed to be  $\tau_2 \sim 1/\delta_d$ . It is clear, however, that there are no grounds for this conclusion in dilute systems. For example, exchange pairs—clusters with spins separated by a distance on the order of the lattice constant—are well known. The interaction in them can exceed 10 GHz appreciably, and in the concentration range of interest to us they are perfectly isolated from the main mass of the impurity.<sup>22</sup> It is natural to assume that the centers that contribute to line wings at  $|\Delta| \lesssim 1$  GHz, i.e., in a position intermediate between exchange pairs and solitary spins, reach quasi-equilibrium with the latter after a certain time  $\tau_{cr} \gg \tau_2$  (Ref. 2).

We assume thus that the spin-spin broadening of the EPR line in a magnetically dilute crystal is in fact inhomogeneous, at least on the far wings. It can be assumed that after a time  $\tau_2 \sim 1/\delta_d$  an internal equilibrium is established only in the "low frequency" part of the subsystem  $\mathcal{H}'_{SS}$ , which corresponds to interaction at distances on the order of  $\bar{r}$ . It is just the temperature  $T_{SS}$  of this system that we determine by measuring the susceptibility signal at the low-frequency  $\Omega \lesssim \delta_d$ .

The remaining (cluster) paramagnetic centers form spin packets located on far wings of the EPR line. We note that even in the simplest case of  $S = 1/2$  spins coupled by dipole interaction the spectrum of an individual pair consists of two lines symmetric about  $\nu_0$  (the "Pake doublet"). Thus, in contrast to the usual inhomogeneous broadening, now each spin packet has at least two spectral components on opposite wings of the line. The width of these components is close to  $\delta_d$ , since it is determined by the amplitude of the fluctuating local fields produced by single spins at the locations of the clusters.

By saturating the EPR line with small detuning  $|\Delta| \sim \delta_d$ , we act directly on the reservoir of the spin-spin interactions of single centers. This leads right away to an increase of the low-frequency susceptibility  $\chi(\Omega)$ . If, however, the microwave pulse is applied to the far wing of the line ( $|\Delta| \gg \delta_d$ ), the main change takes place in the average energy of the interaction in the cluster, an energy that plays the role of the difference subsystem (see § 3a).

Next to act is spectral diffusion, wherein the energy is redistributed among the solitary and cluster spins. This process constitutes establishment of internal equilibrium with a single temperature  $T_{SS}$  in the entire spin-spin system  $\mathcal{H}_{SS}$  as a whole. Judging from our data, it lasts up to times on the order of  $10^{-3}$  sec, which are comparable with  $\tau_{SSL}$ . The stronger the spin-spin interaction and the weaker the spin-lattice interaction, the farther the spectral diffusion manages to advance on the line wings, and this is the cause of the increase of  $\Delta_{\max}^{\infty}$  with increasing  $c$  and with decreasing  $T_L$  (see the table).

The role of the far line wings in the process described above depends substantially on the concrete spin-spin interaction mechanism that predominates in the given substance. Thus for dipole interactions  $\mathcal{H}_{SS} \propto r^{-3}$  and the line shape is close to a truncated Lorentzian. It can be assumed in this case that  $g(\delta) \propto \delta^{-2}$  on the far wings and therefore the specific heats  $c_{\delta} \propto \delta^2 g(\delta)$  of the difference subsystems do not decrease with increase of  $|\delta|$  up to the "cutoff frequency"—a detuning on the order of 2–3 GHz, corresponding to interaction at the shortest distance. This means that the cluster spins, their small number notwithstanding, influence quite appreciably the behavior of the ESSR. If, however, the interaction potential decreases with distance more rapidly than  $r^{-3}$ , the far wings of the lines will have even smaller slopes and the influence even larger.

It must be stated in this connection that the nature of the spin-spin interaction in  $\text{TiO}_2\text{:Cr}^{3+}$  is still not clear enough. At medium distances they are apparently in the main dipole-dipole interactions, as attested by the proximity of  $\delta_{1/2}$  to  $\delta_d$ . As for the far wings of the line, the predominance of exchange or of electric quadrupole forces cannot be excluded here. Arguments in favor of the latter were advanced by Peskovatskii.<sup>21</sup> They are particularly important for rutile, which has an anomalously high dielectric constant ( $\epsilon \sim 100$ ). This raises the question whether the phenomena observed are peculiar only to  $\text{TiO}_2\text{:Cr}^{3+}$  or whether they are typical of a large class of dilute paramagnets.<sup>3)</sup>

#### 4. CONCLUSION

Modern theory of magnetic resonance describes well two stages in the evolution of a spin system: the very earliest ( $t \ll \tau_2$ ), where the purely dynamic approach can be used, and a later one ( $t \gg \tau_2$ ), where spin thermodynamics comes into play. The intermediate stage remains so far practically uninvestigated.

We propose that we have succeeded in the present study in penetrating into this difficultly accessible and, in many respects, puzzling region, where the dynamic description is already unsuitable, but quasi-equilibrium has not yet set in. It was found that in magnetically dilute solids this "troubled time" can be extraordinarily long—sometimes occupying the entire interval from  $\tau_2$  to  $\tau_1$ . No real theory exists as yet, and the physical picture presented in § 3b can be regarded only as a working hypothesis with which to explain the experimental data. For further progress it is necessary to calculate the characteristic time of the process, describe its kinetics and the dependence on the impurity density, etc. We do

not know the location of the boundary between the solitary spins and the cluster spins, meaning the boundary between the first stage of the establishment of the quasi-equilibrium ( $\tau_2$ ) and the second ( $\tau_{cr}$ ). Does a distinct boundary even exist? Or perhaps does the language of spin temperatures become usable only after all the spin-spin processes, and up to then the parameter  $\omega_{SS}$  has no definite value and depends on the observation time? It is also possible that at low impurity densities the spin excitation is localized in clusters, and when  $c$  reaches a certain critical value percolation and a transition to collective behavior takes place.

The results have thus raised a host of new questions concerning fundamental premises of the physics of disordered spin systems. So far, the number of these questions is considerably larger than the number of the answers, so that much work awaits the theoreticians and the experimenters.

The authors thank V. V. Demidov, A. E. Mefed, and M. I. Rodak for help with the work and for valuable advice.

<sup>1</sup>A rigorous theory of the effect of enhanced susceptibility at  $H_0 = 0$  is developed in Ref. 6.

<sup>2</sup>This idea was used earlier in a discussion of the concentration dependence of spin-lattice relaxation.<sup>21,23</sup>

<sup>3</sup>In analogous experiments on ruby<sup>4</sup> the apparatus was not modified to record fast processes. Furthermore, it was difficult there to separate these processes from the effect of the ESSR coupling with the <sup>27</sup>Al nuclei.

<sup>1</sup>V. A. Atsarkin, Zh. Eksp. Teor. Fiz. **64**, 1087 (1973) [Sov. Phys. JETP **37**, 552 (1973)].

<sup>2</sup>V. A. Atsarkin, Fiz. Tverd. Tela (Leningrad) **17**, 2398 (1975) [Sov. Phys. Solid State **17**, 1582 (1975)].

<sup>3</sup>V. A. Atsarkin, O. A. Ryabushkin, and V. A. Skidanov, Zh. Eksp. Teor. Fiz. **72**, 1118 (1977) [Sov. Phys. JETP **45**, 584 (1977)].

<sup>4</sup>V. A. Atsarkin and G. A. Vasneva, Zh. Eksp. Teor. Fiz. **80**, 2098 (1981) [Sov. Phys. JETP **53**, 1094 (1981)].

<sup>5</sup>A. V. Duglav, N. G. Koloskova, B. I. Kochelaev, and A. Kh. Khasanov, Zh. Eksp. Teor. Fiz. **79**, 2367 (1980) [Sov. Phys. JETP **52**, 1199 (1980)].

<sup>6</sup>L. L. Buishvili and I. M. Metreveli, Fiz. Tverd. Tela (Leningrad) **21**, 866 (1979) [Sov. Phys. Solid State **21**, 507 (1979)].

<sup>7</sup>H. J. Gerritsen and S. E. Harrison, J. Appl. Phys. **31**, 1566 (1960).

<sup>8</sup>B. N. Provotorov, Zh. Eksp. Teor. Fiz. **41**, 1582 (1961) [Sov. Phys. JETP **14**, 1126 (1962)].

<sup>9</sup>V. A. Atsarkin and M. I. Rodak, Usp. Fiz. Nauk **107**, 3 (1972) [Sov. Phys. Usp. **15**, 251 (1972)].

<sup>10</sup>M. I. Rodak, Zh. Eksp. Teor. Fiz. **61**, 832 (1971) [Sov. Phys. JETP **34**, 443 (1972)].

<sup>11</sup>V. A. Atsarkin, Dinamicheskaya polarizatsiya yader v tverdykh dielektrikakh (Dynamic Polarization of Nuclei in Solid dielectrics) Nauka, Ch. 6, 1980.

<sup>12</sup>S. Clough and C. A. Scott, J. Phys. C, **1**, 919 (1968).

<sup>13</sup>A. A. Manenkov and A. M. Prokhorov, Zh. Eksp. Teor. Fiz. **42**, 75 (1962) [Sov. Phys. JETP **15**, 54 (1962)].

<sup>14</sup>D. M. Daraseliya, A. S. Epifanov, and A. A. Manenkov, Zh. Eksp. Teor. Fiz. **59**, 445 (1970) [Sov. Phys. JETP **32**, 244 (1971)].

<sup>15</sup>K. S. Yngvesson, IEEE J. of Quantum Electronics **QE-2**, 165 (1966).

<sup>16</sup>L. L. Buishvili, M. D. Zviadadze, and G. R. Khutsishvili, Zh. Eksp. Teor. Fiz. **56**, 290 (1969) [Sov. Phys. JETP **29**, 159 (1969)].

<sup>17</sup>V. A. Atsarkin and V. V. Demidov, Zh. Eksp. Teor. Fiz. **76**, 2185 (1979) [Sov. Phys. JETP **49**, 1104 (1979)].

<sup>18</sup>L. L. Buishvili and M. D. Zviadadze, Phys. Lett. **24A**, 661 (1967).

<sup>19</sup>M. I. Rodak, Zh. Eksp. Teor. Fiz. **79**, 1345 (1980) [Sov. Phys. JETP **52**, 680 (1980)].

<sup>20</sup>W. J. C. Grant and M. W. P. Strandberg, Phys. Rev. **135A**, 715, 727 (1964).

<sup>21</sup>S. A. Peskovatskii, Phys. Stat. Sol. **44**, 543, 551 (1971).

<sup>22</sup>J. C. Gill, Proc. Phys. Soc. **79**, 148 (1962).

<sup>23</sup>V. A. Atsarkin, Zh. Eksp. Teor. Fiz. **49**, 148 (1965) [Sov. Phys. JETP **22**, 106 (1966)].

Translated by J. G. Adashko